Stress Damage in Borehole and Rock Cores; Developing New Tools to Update the Stress Map of Alberta*

Qing Jia[1], Randy Kofman[2], Doug Schmitt[2], and Inga Moeck[3]

Search and Discovery Article #41451 (2014)
Posted October 6, 2014

*Adapted from extended abstract prepared in conjunction with presentation at CSPG/CSEG/CWLS GeoConvention 2013, (Integration: Geoscience engineering Partnership) Calgary TELUS Convention Centre & ERCB Core Research Centre, Calgary, AB, Canada, 6-12 May 2013, AAPG/CSPG©2014

[1]University of Alberta, Edmonton (qjia@ualberta.ca)
[2]University of Alberta, Edmonton
[3]GFZ, Potsdam

Abstract

The *in situ* stress field is the most critical factor in rock mechanics. Different in situ stresses can lead to different rock fractures in terms of types of fracture, apertures, and so on. Therefore, knowledge of fracture information and elastic properties helps us to infer the magnitude and the orientation of the *in situ* stress field. This study shows how to determine the *in situ* stress field in part of Alberta by using this kind of method.

Introduction

As we all know, knowledge of *in situ* stress state enables us to determine the optimum borehole trajectory, evaluate hydrocarbon migration, and so on. Also, the state of stress in the earth is a critical, but often ignored, factor in the success of geothermal energy production. The ability to move fluids through a fractured reservoir is key to the productivity and stress directions and magnitudes will control the *in situ* permeability and fracture geometries. Consequently, it is necessary to understand the state of stress in the earth in order to design and efficiently operate engineered geothermal systems. This need is motivating us to develop a new 3D model of stress for Alberta. The inputs to the model will come from industrial borehole logs and cores and as such there is a strong need to better interpret such observations.

Borehole fractures can be divided into natural fractures and drilling-induced fractures. For natural fractures, they are generated naturally, and they existed before the hole was drilled (Aadnoy and Bell, 1998). Drilling-induced fractures are mainly caused by two kinds of failure mechanisms, which are tensile failure and shear failure, depending on the principal stress state acting on the borehole wall and the elasticity of the failure surface (Aadnoy and Bell, 1998; Thorsen, 2011). Figure 1 shows three main types of drilling induced fractures, which are tensile fracture (left), borehole breakout (middle), and en-echelon E-DITF. This study will investigate the E-DITF initiation and its indication about the stress state. Thus, knowing the orientations and apertures of those fractures can help us better understand the *in situ* stress state.

However, before the fracture analysis, the fundamental step is to know how the stress is distributed around the borehole wall. The co-ordinate for stress concentration around a borehole wall is more convenient to be set in terms of the cylindrical coordinate. As illustrated in Figure 2, the normal stress components generally include σ_{rr}, $\sigma_{\theta\theta}$ and $\sigma_{\zeta\zeta}$, which are the radial, hoop and axial stress, respectively, and $\tau_{\theta\zeta}$, $\tau_{\theta r}$ and $\tau_{r\zeta}$ are shear stresses. For a general case, the stresses at the borehole wall can be expressed as the following:

$$\sigma_{rr} = p_w$$

$$\sigma_{\theta\theta} = \sigma_{xx} + \sigma_{yy} - 2(\sigma_{xx} - \sigma_{yy})\cos 2\theta - 4\tau_{xy} \sin 2\theta - p_w$$

$$\sigma_{\zeta\zeta} = \sigma_{zz} - \nu[2(\sigma_{xx} - \sigma_{yy})\cos 2\theta + 4\tau_{xy} \sin 2\theta]$$

$$\tau_{\zeta r} = \tau_{r\theta} = 0$$

$$\tau_{\theta\zeta} = 2(-\tau_{xz} \sin\theta + \tau_{yz} \cos\theta)$$

where σ_{xx}, σ_{yy}, and σ_{zz} are normal stresses, τ_{xy}, τ_{yz} τ_{xz} and are shear stresses in x-y-z coordinate and p_w is the borehole pressure (Fjaer et al., 2008). When the borehole axis is deviated from the *in situ* principal stresses, we can introduce two Cartesian co-ordinates frames (Figure 2), in which x-y-z having z pointing along the vertical direction, and x'-y'-z' indicating the *in situ* principal stress directions; then, a transformation from x'-y'-z' co-ordinate to x-y-z co-ordinate can be operated by direction cosines (Fjaer et al., 2008; Schmitt et al., 2012). On the other hand, if the borehole axis is aligned with one of the normal stresses, the transformation is not necessary, and all shear stresses will vanish (Aadnoy and Bell, 1998).

The principal stresses at the borehole wall are generally considered as a two dimensional problem since σ_i is always pressing outward of the borehole wall, and they are defined as (Aadnoy and Bell, 1998):

$$\sigma_i = p_w$$

$$\sigma_{j,k} = \tfrac{1}{2}(\sigma_{\theta\theta} + \sigma_{\zeta\zeta}) \pm \tfrac{1}{2}[(\sigma_{\theta\theta} - \sigma_{\zeta\zeta})^2 + 4\tau_{\zeta\theta}{}^2]^{1/2}$$

If there is no shear stress, the principal stresses equal to the axial and hoop stress; however, if the shear stresses exist, it leads to the rotation of the principal stresses with an angle β, which has the following expression:

$$\beta = \arccos\left[\frac{\sigma_{\theta\zeta}}{[(\sigma_{\theta\theta} - \sigma_{min})^2 + \tau_{\theta\zeta}{}^2]^{1/2}}\right]$$

where is the minimum principal stress (Aadnoy, 1990).

Regarding to failure mechanisms, high well pressure tends to generate tensile failures ($\sigma_i > \sigma_{j,k}$), and can be considered as a crack (generally higher conductivity in FMS log) (Aadnoy and Bell, 1998; Thorsen, 2011; Davatzes and Hickman, 2010). On the contrary, low well pressure usually leads to compressive failure ($\sigma_j > \sigma_i$) resulting in borehole breakout (Aadnoy and Bell, 1998; Thorsen, 2011).

This study first focuses on modeling near-wellbore stress concentration (hoop stress, axial stress, radial stress, etc.) in an isotropic, homogeneous formation and analyzing principles of failure mechanisms around the borehole wall. Based on these analyses, fracture geometry, which is determined in terms of both principal stress magnitudes and its orientation with respect to the borehole trajectory, can be modeled. And the second step is to investigate stress distributions around the borehole in an anisotropic formation.

In addition, to achieve elastic properties, laboratory strength tests will be conducted on selected cores, which can show different fracture surfaces under different stress states. Furthermore, natural and drilling-induced fractures identified from wellbore image data and the comprehensive well logging information enable us to evaluate the stress field in Alberta more accurately.

Theory and/or Method

To visualize how stress concentration changes at different distances r from the borehole axis and at different azimuths with respect to y-axis, except for those two co-ordinates (x-y-z and x'-y'-z') which were mentioned above, we introduce the third r-θ-ζ co-ordinate, and the borehole axis is aligned with ζ-axis (Figure 2) (Schmitt et al., 2012). This model was first created by Hiramatsu and Oka (1962), and stresses around the borehole wall are written as the following:

$$\sigma_{rr} = \alpha_1\left(1 - \frac{a^2}{r^2}\right) + \alpha_2\left(1 - 4\frac{a^2}{r^2} + 3\frac{a^4}{r^4}\right)\cos 2\theta + \alpha_3\left(1 - 4\frac{a^2}{r^2} + 3\frac{a^4}{r^4}\right)\sin 2\theta$$

$$\sigma_{\theta\theta} = \alpha_1\left(1 + \frac{a^2}{r^2}\right) + \alpha_2\left(-1 - 3\frac{a^4}{r^4}\right)\cos 2\theta + \alpha_3\left(-1 - 3\frac{a^4}{r^4}\right)\sin 2\theta$$

$$\tau_{\zeta\zeta} = \beta_1 - 4\upsilon\left(\alpha_2\frac{a^2}{r^2}\cos 2\theta + \alpha_3\frac{a^2}{r^2}\sin 2\theta\right)$$

$$\tau_{\theta\zeta} = \gamma_1\left(1 + \frac{a^2}{r^2}\right)\cos\theta + \gamma_2\left(1 + \frac{a^2}{r^2}\right)\sin\theta$$

$$\tau_{r\zeta} = \gamma_1\left(1 - \frac{a^2}{r^2}\right)\sin\theta - \gamma_2\left(1 - \frac{a^2}{r^2}\right)\cos\theta$$

$$\tau_{r\theta} = \alpha_2\left(-1 - 2\frac{a^2}{r^2} + 3\frac{a^4}{r^4}\right)\sin 2\theta + \alpha_3\left(1 + 2\frac{a^2}{r^2} - 3\frac{a^4}{r^4}\right)\cos 2\theta$$

where ν is Poisson's ratio, α_1, α_2, α_3, β_1, γ_1 and γ_2 are the coefficients as a function of direction cosines, in situ stress magnitudes and the inclination ϕ of the borehole axis. Then we created a MATLAB code that can show the distribution of stress around and on the borehole wall in a linear elastic, isotropic and homogeneous formation under different *in situ* stress states (Figure 4). Furthermore, principal stresses were also calculated to simulate fracture geometry (Figure 5).

Those equations above imply that when the borehole axis is aligned with the vertical principal stress, maximum concentrated compression of hoop stress (red area) occurs at the angle of 90°with respect to $\boldsymbol{\sigma_{x'x'}}$, and that is where the borehole breakout tends to grow. Moreover, minimum concentrated compression of hoop stress, which is at the same direction as $\boldsymbol{\sigma_{x'x'}}$, is the place where tensile fracture tends to occur (Figure 3). Therefore, we can make advantage of image log to constrain *in-situ* stress orientations.

Examples

For a borehole wall in a linear elastic, isotropic, and homogeneous formation, the top of Figure 4 illustrates the distribution of hoop stress (left), axial stress (middle), and radial stress concentration (right) around a vertical borehole, and in this case, $\boldsymbol{\sigma_{x'x'}}$=30MPa, $\boldsymbol{\sigma_{y'y'}}$ =10MPa, $\boldsymbol{\sigma_{z'z'}}$=100MPa, p_w=10MPa, and ν=0.25; moreover, the bottom of Figure 4 demonstrates the stress concentration around a deviated borehole (ϕ = 45 degree, azimuth with respect to $\boldsymbol{\sigma_{x'x'}}$=45 degree) under the same *in situ* stress condition. In addition, Figure 5 shows corresponding principal stresses acting on the borehole wall. The result confirms that a deviated borehole can rotate stresses leading to nonalignment drilling induced fractures.

Aside from the stress concentration model, Figure 1 shows the borehole televiewer data from the southern part of Idaho that James Kessler is working on. The left side shows drilling induced tensile fracture, and it occurs at the angle of 90° with respect to the minimum horizontal stress at depth interval 4370 ft to 4375 ft. The right side shows a planar feature (red curve), and it could be a natural fracture, a fault and so on. What in the yellow boxes are borehole breakouts indicating the direction of minimum horizontal stress.

Conclusions

Results show that drilling induced fractures are likely to grow normal to the maximum horizontal stress where it is more tensile and borehole breakouts are likely to grow normal to the minimum horizontal stress where it is more compressive when borehole is aligned with in-situ stress. On the other hand, when the borehole is deviated, the tensile fracture should be expected to occur in a nonalignment direction with respect to the borehole axis.

Acknowledgements

This work is supported by Helmholtz-Alberta Initiative. James Kessler's assistance in providing image log data is greatly appreciated.

References Cited

Aadnoy, B., 1990, In-situ stress directions from borehole fracture traces: Journal of Petroleum Science and Engineering, v. 4, p. 143-153.

Aadnoy, B., and J. Bell, 1998, Classification of drilling-induced fractures and their relationship to in-situ stress directions: The Log Analyst, p. 27-42.

Davatzes, N., and S. Hickman, 2010, Stress, fracture, and fluid-flow analysis using acoustic and electrical image logs in hot fractured granites of the Coso geothermal field, California, U.S.A. *in* M. Pöppelreiter, C. Garcia-Carballido, and M. Kraaijveld, (eds.), Dipmeter and Borehole Image Log Technology: American Association of Petroleum Geologists, p. 259–293.

Fjaer, E., R. Holt, P. Horsrud, A. Raaen, and R. Risnes, 2008, Petroleum related rock mechanics: Elsevier, Amsterdam, 2nd ed., 514 p.

Hiramatsu, Y., and Y. Oka, 1962, Stress around a shaft or level excavated in ground with a three-dimensional stress state: Memoirs of the Faculty of Engineering, Kyoto University Part I, v. 24, p. 56-76.

Schmitt, D., C. Currie, and L. Zhang, 2012, Crustal stress determination from boreholes and rock cores: Fundamental principles: Tectonophysics, v. 580, p. 1-26, http://dx.doi.org/10.1016/j.tecto.2012.08.029.

Thorsen, K., 2011, In situ stress estimation using borehole failures – Even for inclined stress tensor: Journal of Petroleum Science and Engineering, v. 79, p. 86-100.

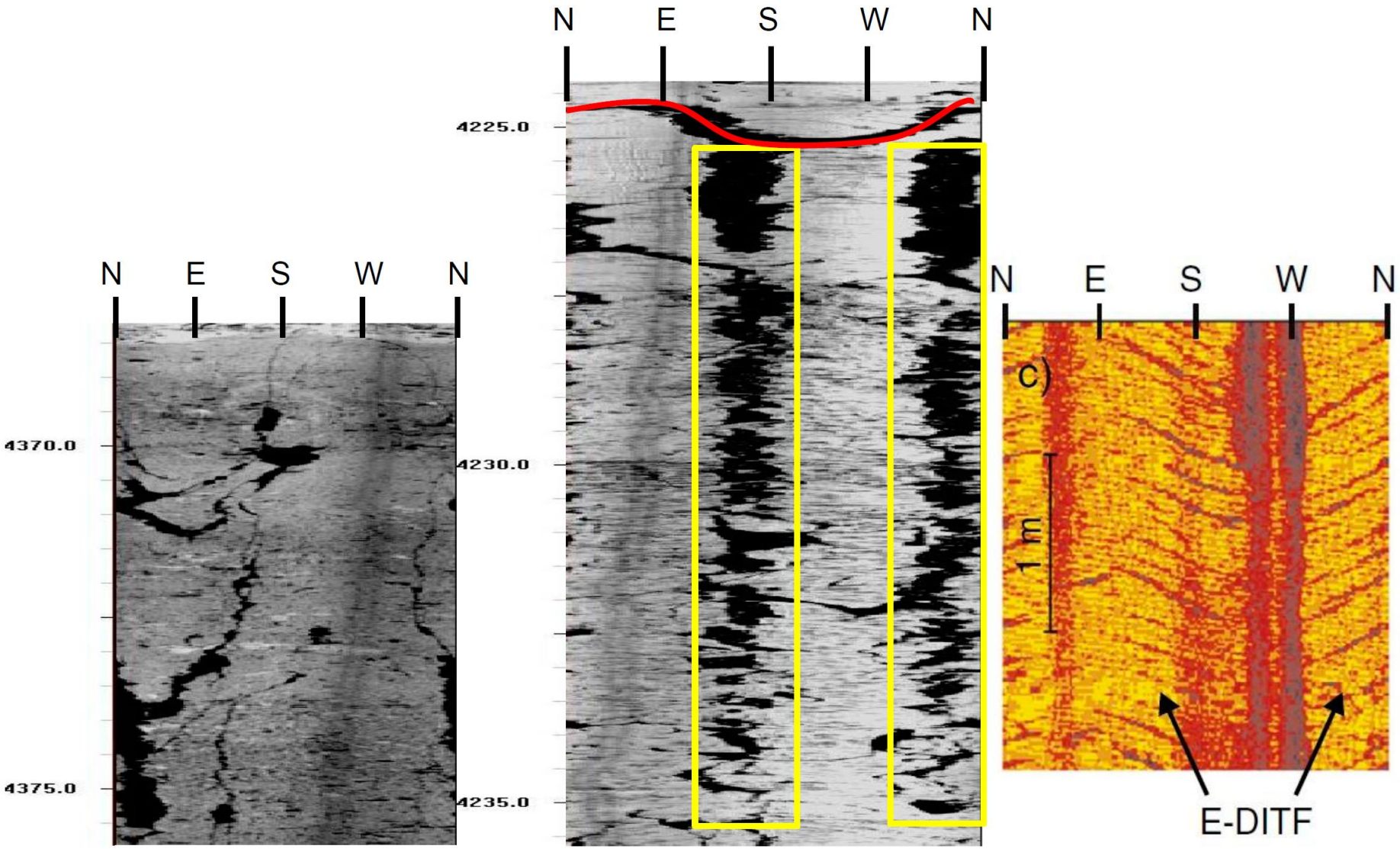

Figure 1. Left: Borehole televiewer image data from southern Idaho shows tensile fracture; middle: the same data set as the left one, which shows planar feature (red line) and borehole breakouts (yellow boxes); right: an example of en-echelon or chevron (E-DITF) pattern.

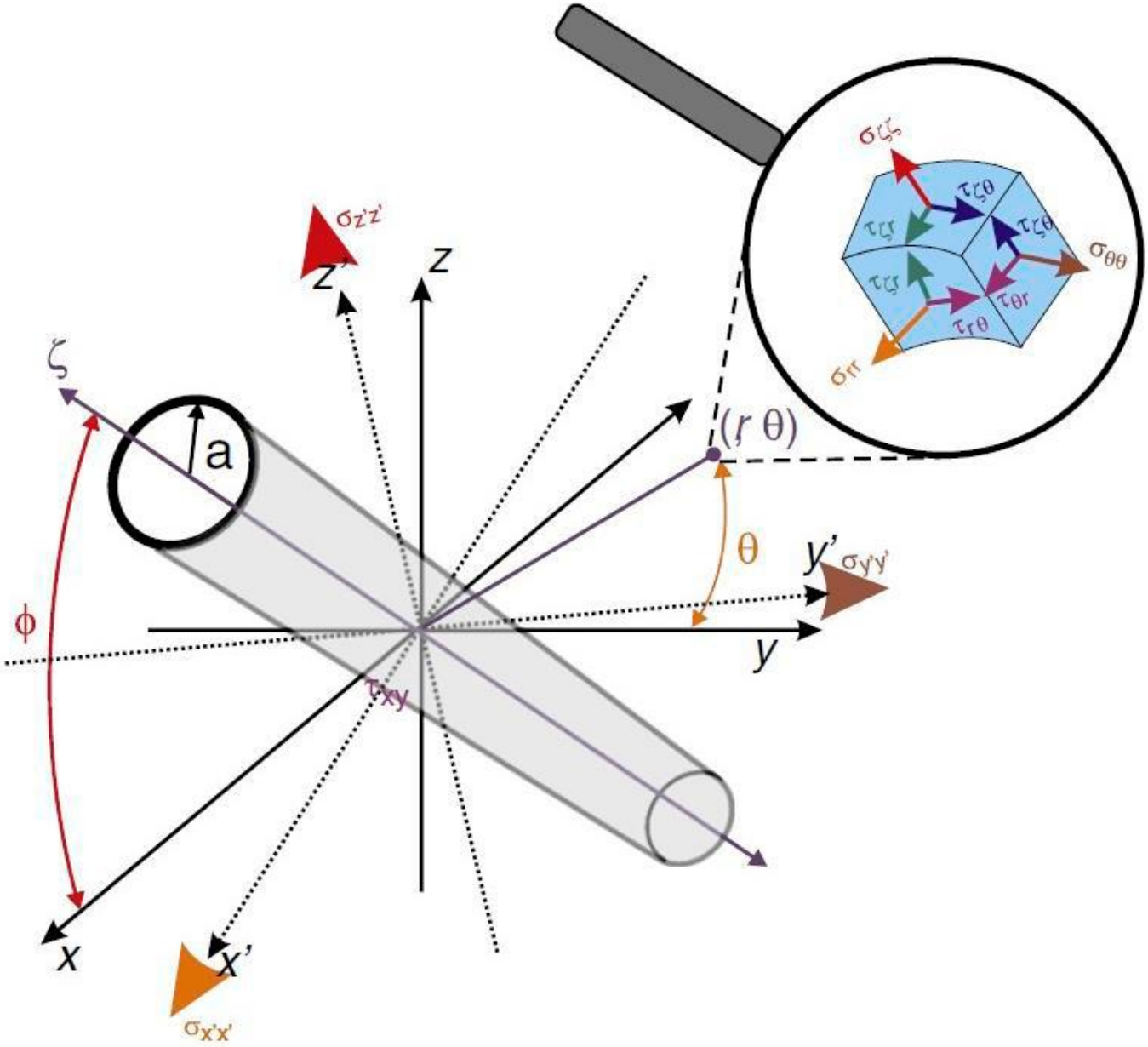

Figure 2. Stresses acting on the borehole wall and different coordinate frames (Schmitt et al., 2012).

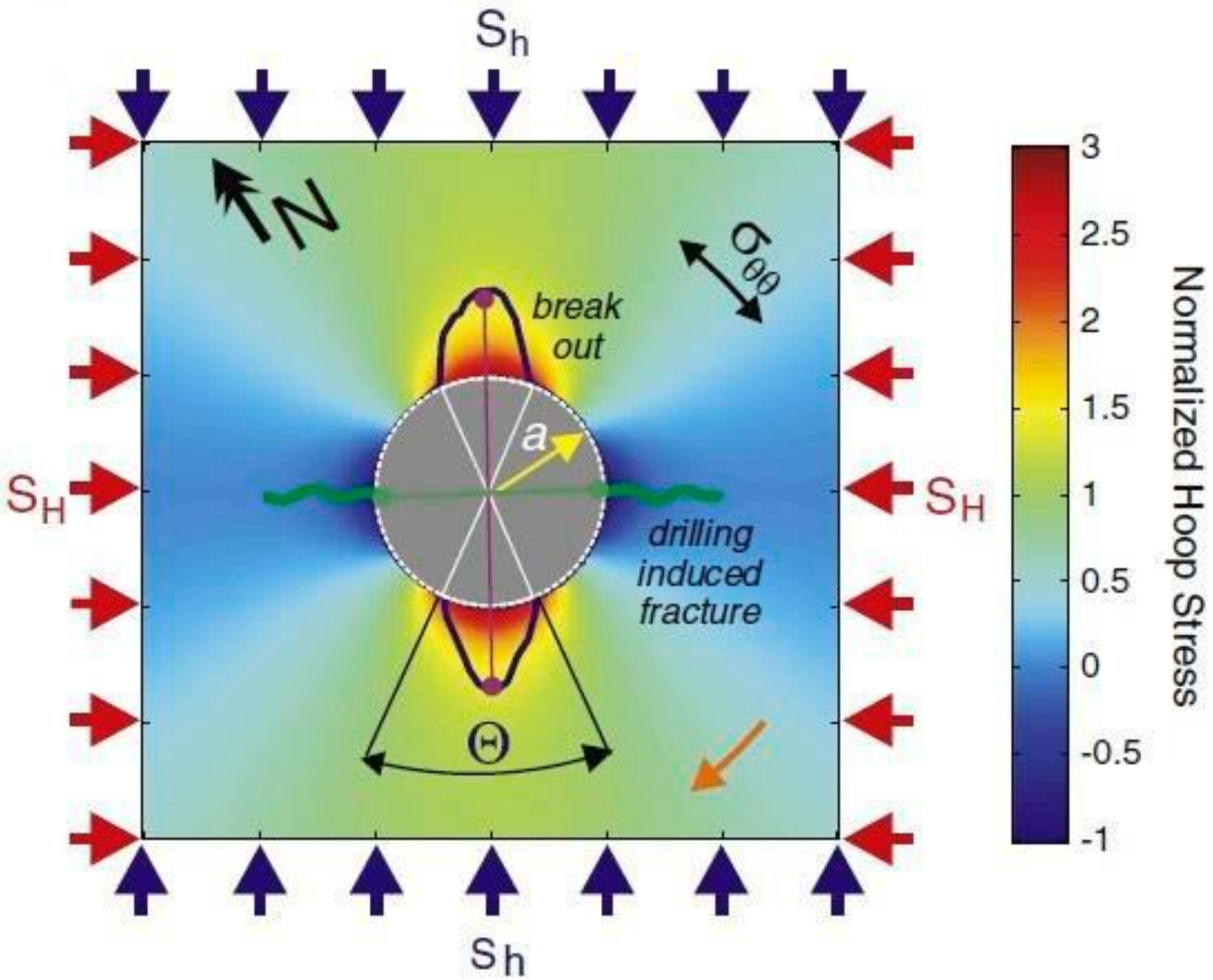

Figure 3. Stress induced borehole deformation (Schmitt et al., 2012).

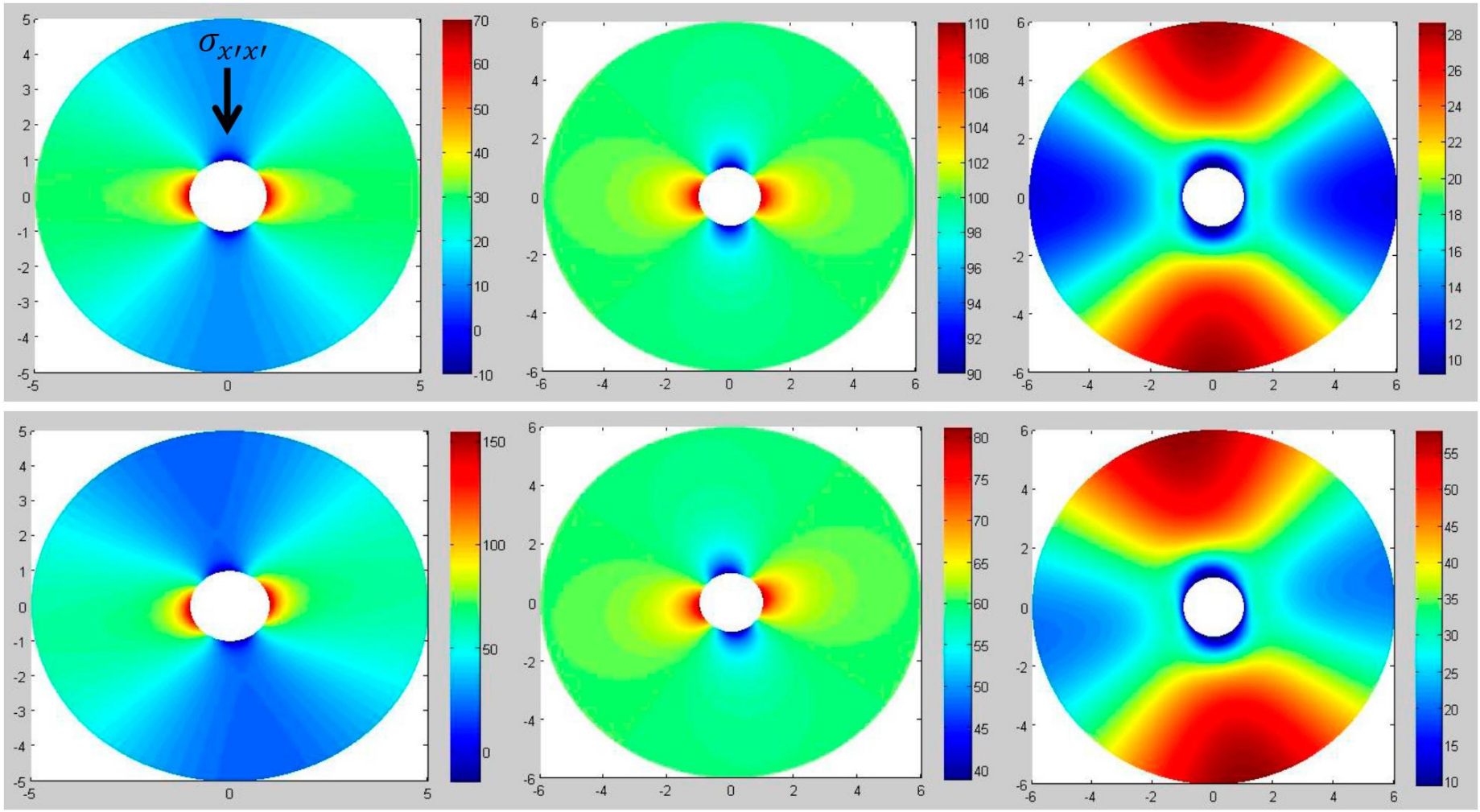

Figure 4. Stress concentration around a vertical (top) and deviated (bottom) borehole wall.

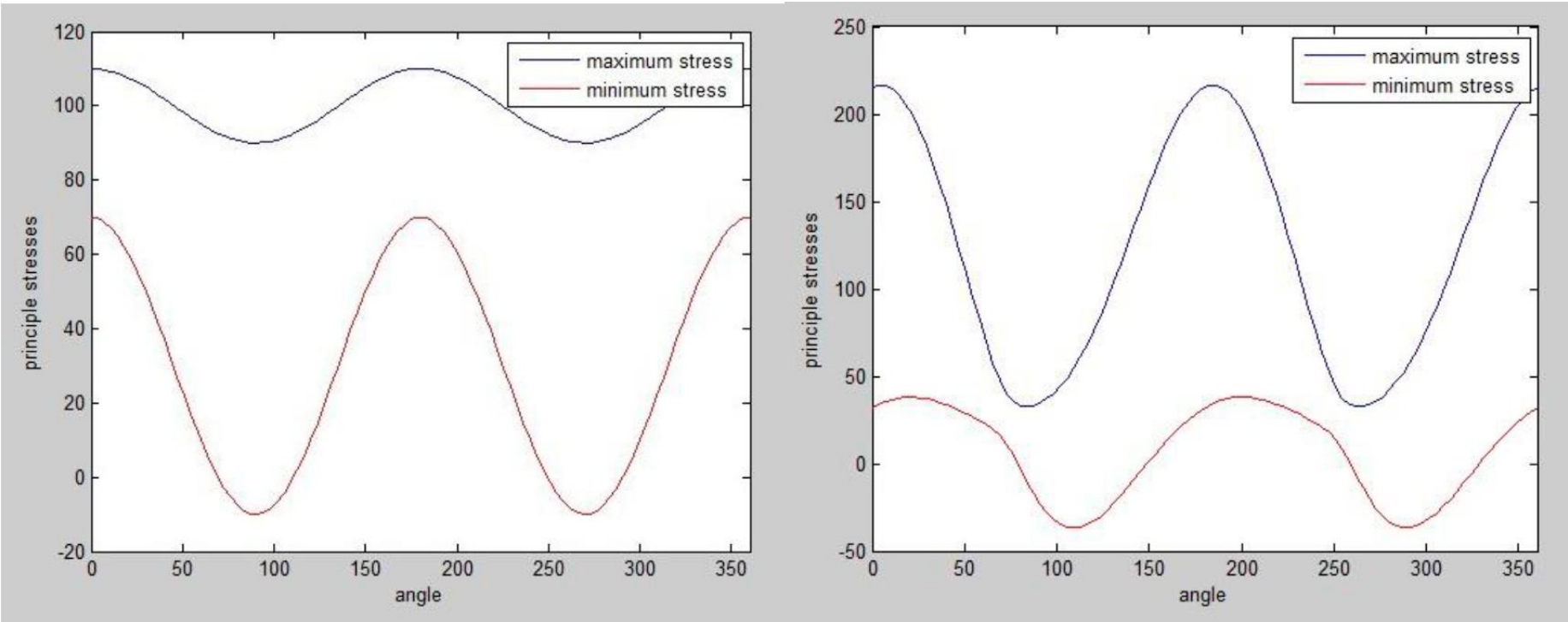

Figure 5. Principal stresses acting on a borehole wall when (left) the borehole is aligned with in-situ stresses and (right) the borehole is deviated from in-situ stresses.